

C-Terminal Fragment, $A\beta_{32-37}$, Analogues Protect Against $A\beta$ Aggregation-Induced Toxicity

Sunil Bansal,[†] Indresh Kumar Maurya,[‡] Nitin Yadav,[§] Chaitanya Kumar Thota,[§] Vinod Kumar,^{||} Kulbhushan Tikoo,^{||} Virander Singh Chauhan,[§] and Rahul Jain^{*,†}

[†]Department of Medicinal Chemistry, National Institute of Pharmaceutical Education and Research, Sector 67, S.A.S Nagar 160 062, Punjab India

[‡]Department of Microbial Biotechnology, Panjab University, Sector 14, Chandigarh 160 014, India

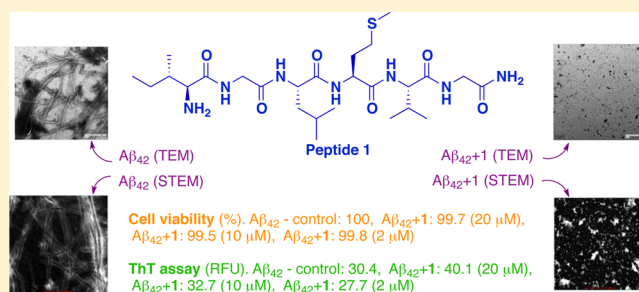
[§]International Center for Genetic Engineering and Biotechnology, Aruna Asif Ali Marg, New Delhi 110 067, India

^{||}Department of Pharmacology and Toxicology, National Institute of Pharmaceutical Education and Research, Sector 67, S.A.S Nagar 160 062, Punjab India

Supporting Information

ABSTRACT: Amyloid- β aggregation is a major etiological phenomenon in Alzheimer's disease. Herein, we report peptide-based inhibitors that diminish the amyloid load by obviating $A\beta$ aggregation. Taking the hexapeptide fragment, $A\beta_{32-37}$, as lead, more than 40 new peptides were synthesized. Upon evaluation of the newly synthesized hexapeptides as inhibitors of $A\beta$ toxicity by the MTT-based cell viability assay, a number of peptides exhibited significant $A\beta$ aggregation inhibitory activity at sub-micromolar concentration range. A hexapeptide (**1**) showed complete mitigation of $A\beta$ toxicity in the cell culture assay at 2 μ M. In the ThT fluorescence assay, upon incubation of $A\beta$ with this peptide, we observed no increase in the ThT fluorescence relative to control. The secondary structure estimation by circular dichroism spectroscopy and morphological examination by transmission electron microscopy further confirmed the results.

KEYWORDS: Alzheimer's disease, $A\beta$ aggregation, hexapeptide, MTT, ThT fluorescence assay, TEM



Ever since it was reported by Alois Alzheimer more than a century ago,¹ Alzheimer's disease (AD) has grown exponentially in terms of affected cases, all over the world. AD is one of the most common forms of dementia that stems from the abnormal accumulation of $A\beta$ and tau proteins into senile plaques and neurofibrillary tangles, respectively. The number of people living with dementia worldwide today is estimated at 44 million; set to almost double (75.6 million) by 2030 and more than triple (135.5 million) by 2050.² Such an ever increasing number of patients would challenge society on social, medical, and economical fronts. Neuropathology, genetics, and transgenic modeling studies have evidenced the key role of $A\beta$ peptides in the etiology of AD.³ $A\beta$ is generated by sequential cleavage of amyloid precursor protein (APP) by the action of enzymes, β - and γ -secretases.⁴ $A\beta$ peptide, that normally exists as unordered, in the form of a random coil, exhibits a transition toward cross- β -sheet pattern in abnormal conditions, ultimately resulting in its deposition as plaques around the neuronal cells.⁵ Understanding of the disease mechanism and etiology has helped scientists to identify a number of potential targets to combat this disease.

The first pharmacological approach used to treat Alzheimer's disease was based on the use of acetyl cholinesterase (AChE)

inhibitors. The United States Food and Drug Administration (FDA) approved AChE inhibitors such as tacrine, donepezil, rivastigmine and galantamine, and the *N*-methyl-D-aspartate (NMDA)-receptor antagonist memantine, mainly provide symptomatic relief and do not reverse or prevent the progression of the disease.⁶ Though a number of compounds targeting β - or γ -secretases are currently in clinical trials,^{7,8} many of such compounds have failed recently.^{9–11} Similarly, most of the immunotherapies have shown improvements in cognitive function and reduction in $A\beta$ load,^{12,13} but the adverse events are still the issues to be resolved. Chelation therapies developed to disrupt the interactions between $A\beta$ and metals once attracted considerable attention; however, the only metal chelators, PBT1 and PBT2, tested in clinical trials have failed.^{14,15} The approaches based on tau protein regulation have not yielded many therapeutically important molecules and only one, phenothiazine methylene blue that acts as aggregation inhibitor of tau protein has been tested in phase III clinical trials.¹⁶ Davunetide, an octapeptide (NAPVSIPQ), has also

Received: January 6, 2016

Accepted: February 2, 2016

Published: February 2, 2016

Table 1. Sequence, HRMS, and HPLC Data of the Synthesized Peptides

peptide no.	sequence	mol formula (mol wt)	HRMS data		HPLC data	
			calcd	obsd	t_R (min)	purity (%)
1	Ile-Gly-Leu-Met-Val-Gly-NH ₂	C ₂₆ H ₄₉ N ₇ O ₆ S (587.3465)	588.3543	588.3543	29.37	97.2
2	Val-Gly-Leu-Met-Val-Gly-NH ₂	C ₂₅ H ₄₇ N ₇ O ₆ S (573.3309)	574.3387	574.3395	27.44	97.5
3	Leu-Gly-Leu-Met-Val-Gly-NH ₂	C ₂₆ H ₄₉ N ₇ O ₆ S (587.3465)	588.3543	588.3543	24.38	100
4	Aib-Gly-Leu-Met-Val-Gly-NH ₂ ^a	C ₂₄ H ₄₅ N ₇ O ₆ S (559.3152)	560.3230	560.3236	25.33	98.6
5	Pro-Gly-Leu-Met-Val-Gly-NH ₂	C ₂₅ H ₄₅ N ₇ O ₆ S (571.3152)	572.3230	572.3231	25.33	97.9
6	Phe-Gly-Leu-Met-Val-Gly-NH ₂	C ₂₉ H ₄₇ N ₇ O ₆ S (621.3309)	622.3387	622.3388	31.81	98.7
7	Ala-Gly-Leu-Met-Val-Gly-NH ₂	C ₂₃ H ₄₇ N ₇ O ₆ S (545.2996)	546.3074	546.3074	25.21	99.2
8	Nva-Gly-Leu-Met-Val-Gly-NH ₂ ^a	C ₂₅ H ₄₇ N ₇ O ₆ S (573.3309)	574.3387	574.3407	23.50	95.5
9	Nle-Gly-Leu-Met-Val-Gly-NH ₂ ^a	C ₂₆ H ₄₉ N ₇ O ₆ S (587.3465)	588.3543	588.3544	26.16	99.0
10	Ile-Val-Leu-Met-Val-Gly-NH ₂	C ₂₉ H ₅₅ N ₇ O ₆ S (629.3935)	630.4013	630.4026	26.26	98.5
11	Ile-Leu-Leu-Met-Val-Gly-NH ₂	C ₃₀ H ₅₇ N ₇ O ₆ S (643.4091)	644.4169	644.4168	29.40	97.5
12	Ile-Aib-Leu-Met-Val-Gly-NH ₂	C ₂₈ H ₅₃ N ₇ O ₆ S (615.3778)	616.3856	616.3856	40.46	99.4
13	Ile-Ile-Leu-Met-Val-Gly-NH ₂	C ₃₀ H ₅₇ N ₇ O ₆ S (643.4091)	644.4169	644.4178	27.80	100
14	Ile-Phe-Leu-Met-Val-Gly-NH ₂	C ₃₃ H ₅₅ N ₇ O ₆ S (677.3935)	678.4013	678.4019	15.53	97.7
15	Ile-Ala-Leu-Met-Val-Gly-NH ₂	C ₂₇ H ₅₁ N ₇ O ₆ S (601.3622)	602.3700	602.3711	24.96	96.9
16	Ile-Nle-Leu-Met-Val-Gly-NH ₂	C ₃₀ H ₅₇ N ₇ O ₆ S (643.4091)	644.4169	644.4169	29.42	99.2
17	Ile-Gly-Pro-Met-Val-Gly-NH ₂	C ₂₅ H ₄₅ N ₇ O ₆ S (571.3152)	572.3230	572.3242	19.85	99.4
18	Ile-Gly-Phe-Met-Val-Gly-NH ₂	C ₂₉ H ₄₇ N ₇ O ₆ S (621.3309)	622.3387	622.3387	25.14	95.7
19	Ile-Gly-Ile-Met-Val-Gly-NH ₂	C ₂₆ H ₄₉ N ₇ O ₆ S (587.3465)	588.3543	588.3543	24.16	96.7
20	Ile-Gly-Val-Met-Val-Gly-NH ₂	C ₂₅ H ₄₇ N ₇ O ₆ S (573.3309)	574.3387	574.3387	21.27	98.6
21	Ile-Gly-Aib-Met-Val-Gly-NH ₂	C ₂₄ H ₄₅ N ₇ O ₆ S (559.3152)	560.3230	560.3230	19.80	99.4
22	Ile-Gly-Ala-Met-Val-Gly-NH ₂	C ₂₃ H ₄₃ N ₇ O ₆ S (545.2996)	546.3074	546.3074	17.41	98.2
23	Ile-Gly-Nle-Met-Val-Gly-NH ₂	C ₂₆ H ₄₉ N ₇ O ₆ S (587.3465)	588.3543	588.3524	25.37	99.7
24	Ile-Gly-Nva-Met-Val-Gly-NH ₂	C ₂₅ H ₄₇ N ₇ O ₆ S (573.3309)	574.3387	574.3387	22.03	99.1
25	Ile-Gly-Leu-Cys-Val-Gly-NH ₂	C ₂₄ H ₄₅ N ₇ O ₆ S (559.3152)	560.3230	560.3237	23.13	97.1
26	Ile-Gly-Leu-Ser-Val-Gly-NH ₂	C ₂₄ H ₄₅ N ₇ O ₇ (543.3380)	544.3458	544.3458	21.03	98.9
27	Ile-Gly-Leu-D-Cys-Val-Gly-NH ₂	C ₂₄ H ₄₅ N ₇ O ₆ S (559.3152)	560.3230	560.3272	25.13	95.6
28	Ile-Gly-Leu-D-Ser-Val-Gly-NH ₂	C ₂₄ H ₄₅ N ₇ O ₇ (543.3380)	544.3458	544.3456	19.95	98.8
29	Ile-Gly-Leu-Met-Pro-Gly-NH ₂	C ₂₆ H ₄₇ N ₇ O ₆ S (585.3309)	586.3387	586.3387	23.90	95.7
30	Ile-Gly-Leu-Met-Phe-Gly-NH ₂	C ₃₀ H ₄₉ N ₇ O ₆ S (635.3465)	636.3543	636.3555	29.37	97.8
31	Ile-Gly-Leu-Met-Ile-Gly-NH ₂	C ₂₇ H ₅₁ N ₇ O ₆ S (601.3622)	602.3700	602.3700	27.04	95.5
32	Ile-Gly-Leu-Met-Leu-Gly-NH ₂	C ₂₇ H ₅₁ N ₇ O ₆ S (601.3622)	602.3700	602.3700	27.92	98.1
33	Ile-Gly-Leu-Met-Aib-Gly-NH ₂	C ₂₅ H ₄₇ N ₇ O ₆ S (573.3309)	574.3387	574.3445	23.97	99.5
34	Ile-Gly-Leu-Met-Ala-Gly-NH ₂	C ₂₄ H ₄₅ N ₇ O ₆ S (559.3152)	560.3230	560.3230	22.21	97.0
35	Ile-Gly-Leu-Met-Nva-Gly-NH ₂	C ₂₆ H ₄₉ N ₇ O ₆ S (587.3465)	588.3543	588.3609	25.62	99.6
36	Ile-Gly-Leu-Met-Nle-Gly-NH ₂	C ₂₇ H ₅₁ N ₇ O ₆ S (601.3622)	602.3700	602.3701	28.50	95.2
37	Ile-Gly-Leu-Met-Val-Phe-NH ₂	C ₃₃ H ₅₅ N ₇ O ₆ S (677.3935)	678.4013	678.4014	33.77	97.1
38	Ile-Gly-Leu-Met-Val-Nle-NH ₂	C ₃₀ H ₅₇ N ₇ O ₆ S (643.4091)	644.4169	644.4172	32.66	95.8
39	Ile-Gly-Leu-Met-Val-Ile-NH ₂	C ₃₀ H ₅₇ N ₇ O ₆ S (643.4091)	644.4169	644.4169	31.09	98.7
40	Ile-Gly-Leu-Met-Val-Leu-NH ₂	C ₃₀ H ₅₇ N ₇ O ₆ S (643.4091)	644.4169	644.4169	31.75	97.3
41	Ile-Gly-Leu-Met-Val-Val-NH ₂	C ₂₉ H ₅₅ N ₇ O ₆ S (629.3935)	630.4013	630.4015	28.48	99.2
42	Ile-Gly-Leu-Met-Val-Aib-NH ₂	C ₂₈ H ₅₃ N ₇ O ₆ S (615.3778)	616.3856	616.3857	27.24	99.1
43	Ile-Gly-Leu-Met-Val-Ala-NH ₂	C ₂₇ H ₅₁ N ₇ O ₆ S (601.3622)	602.3700	602.3701	25.52	98.5
	Ac- β ₃₂₋₃₇ -NH ₂	Ac-Ile-Gly-Leu-Met-Val-Gly-NH ₂				
	β ₁₋₄₂	AEFRHDDSSGYEVHHQKLVFFAEDVGSNKGAIIGLMVGGVVIA				

^aAmino acid denotations: Aib, aminoisobutyric acid; Nle, norleucine; Nva, norvaline.

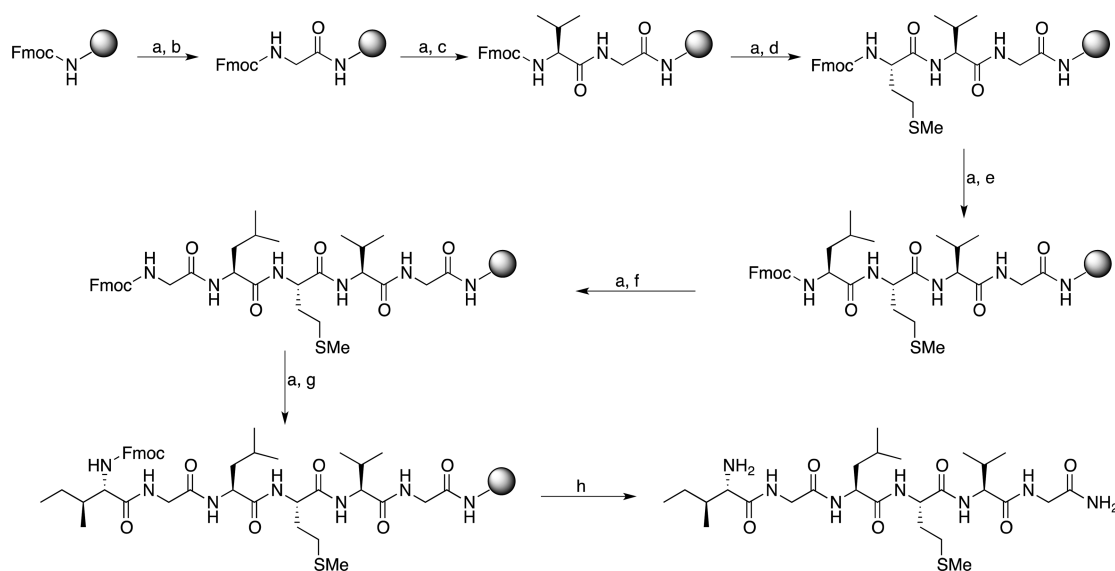
shown benefits in phase II clinical trials for mild cognitive impairment.¹⁷

Inadequate success in the design of anti-AD therapeutics using the above-described approaches and the suggested positive modulatory role of $A\beta$ in neurotransmission and memory¹⁸ led neuroscientists to focus on the design of $A\beta$ aggregation inhibitors. A variety of small molecules such as curcumin,¹⁹ RS0406,²⁰ and some polyphenols²¹ have been reported to interfere with $A\beta$ aggregation, and some even reached in clinical developmental phases.^{22,23} Epigallocatechin-3-gallate (EGCG) is currently undergoing phase III clinical trials against early stages of Alzheimer's disease.²⁴ However, the

inhibition mechanisms of small organic compounds are not clearly understood and majority of them bind to $A\beta$ with no selectivity, hampering their further developments.

Since $A\beta$ is known to bind to itself with great specificity, the parent peptide itself serves as lead in the form of its fragments that could be modified to design inhibitors of the self-assembly of the parent peptide. In recent years, many modified peptides and peptidomimetics derived from the central hydrophobic $A\beta$ sequence have been synthesized as inhibitors of $A\beta$ aggregation.²⁵⁻³⁰ A pentapeptide, SEN606, designed by the N-methylation approach, has undergone preclinical drug developmental phases. A D-enantiomeric pentapeptide, PPI-

Scheme 1. Representative Synthetic Scheme for the C-Terminus Amidated Hexapeptides on the Rink Amide MBHA Resin Exemplified by Peptide 1^a



^aReagents and conditions: (a) 20% piperidine in DMF, 15 min; (b) Fmoc-Gly-OH, TBTU, DIEA, DMF, 2.5 h; (c) Fmoc-Val-OH, TBTU, DIEA, DMF, 2.5 h; (d) Fmoc-Met-OH, TBTU, DIEA, DMF, 2.5 h; (e) Fmoc-Leu-OH, TBTU, DIEA, DMF, 2.5 h; (f) Fmoc-Gly-OH, TBTU, DIEA, DMF, 2.5 h; (g) Fmoc-Ile-OH, TBTU, DIEA, DMF, 2.5 h; (h) TFA, triisopropylsilane, water, 2.5 h.

1019 (Apan), based on the $A\beta_{17-21}$ fragment, developed by Praecis pharmaceuticals has completed phase II clinical trials in humans.³¹ In 2008, Bitan and co-workers prepared a series of $A\beta_{1-42}$ C-terminal fragments ($A\beta_{x-42}$; $x = 28-39$). In their study, $A\beta_{31-42}$ and $A\beta_{39-42}$ were identified as the most effective inhibitors of $A\beta_{1-42}$ -induced toxicity.³² In a report, *N*-methylated hexapeptides based on fragment $A\beta_{32-37}$, protected on both N- and C-terminus were shown to be efficient inhibitors of $A\beta$ aggregation.³³ However, since the last FDA approved drug in 2003, there is not much to highlight in the currently ongoing research for AD therapeutics. Most of the discovered molecules, after showing benefits initially, could not proceed beyond phase II, and very few have progressed to phase III clinical trials. The increasing number of patients and the related social and economical burden create an urgent need to discover newer therapeutics.

LEAD PEPTIDE AND THE RATIONALE

A substantial body of evidence suggests that the hydrophobic C-terminus of $A\beta$ plays a key role in controlling its self-aggregation.³⁴ Since hydrophobic interactions are known to play an important role in protein aggregation,³⁵ the molecules that possess high binding affinity for the C-terminus of $A\beta$ may disrupt the aggregate formation and diminish the neurotoxicity exerted by $A\beta$ aggregates. Therefore, the designing of $A\beta$ fragment-based aggregation inhibitors, though, started from the central hydrophobic sequence ($A\beta_{16-22}$), the focus in the recent years has shifted to the more hydrophobic, and thus, faster aggregating C-terminus region. Many laboratories have utilized the C-terminus of $A\beta$ to design the inhibitors of $A\beta$ assembly; however, the region still remains relatively unexplored. We support the envision put forth by a number of laboratories that the sequestration of β -amyloid monomer association in order to disrupt the fibrillation could be the strategy to combat AD. Peptide-based aggregation inhibitors designed as variants of C-terminus fragments could bind to the parent peptide with more affinity than the $A\beta$ monomers themselves and thus may

preclude amyloid formation. A number of findings that accentuate on the role of C-terminus in $A\beta$ aggregation made the C-terminal region as our sequence of interest. We picked the hexapeptide fragment $A\beta_{32-37}$, from C-terminus of $A\beta$ and performed a full peptide scan. The peptide scan involved the replacement of all the six amino acids by their isosterically analogous amino acids of both natural and unnatural origin, and 42 new peptides were synthesized (Table 1). Peptides were synthesized by fluorenylmethoxycarbonyl (Fmoc) chemistry using standard solid phase peptide synthesis protocol. Scheme 1 represents the general route for the synthesis of C-terminally amidated hexapeptides on the rink amide MBHA resin. Accordingly, rink amide MBHA resin was swelled and Fmoc group was removed using 20% piperidine in DMF. The free amino group containing resin was coupled with amino acids in the presence of TBTU in DMF for 2.5 h. The coupling reaction was monitored by Kaiser's test. After synthesis of the desired chain length, Fmoc group was removed as described earlier. The peptide was delinked from the solid support by using a cleavage cocktail of triisopropylsilane in TFA and water. The crude peptides were purified and their purity was analyzed (see Supporting Information).

RESULTS AND DISCUSSION

MTT Cell Viability Assay. The $A\beta_{32-37}$ -fragment derivative, Ac-Ile-Gly-Leu-Met-Val-Gly-NH₂ (Ac- $A\beta_{32-37}$ -NH₂), protected on both termini was previously reported as mildly active against the $A\beta$ toxicity.³³ However, poly-*N*-methylated analogues based on this sequence were reported to be potent inhibitors of $A\beta$ fibrillation.³³ The designed hexapeptide analogues reported herein are based on the same hexapeptide sequence but with the free N-terminus. Being analogous to a fragment ($A\beta_{32-37}$, i.e., IGLMVG) of the parent peptide itself, the hexapeptides are supposed to have high affinity for $A\beta$ and prevent $A\beta$ -induced toxicity. The initial screening of newly synthesized hexapeptides for anti- $A\beta$ aggregation activity was performed by MTT cell viability assay to assess their effects on the viability of PC-12

cells against the cytotoxicity of aggregating $A\beta$ peptides. Rat pheochromocytoma (PC-12) cells have previously been developed as a model for neuronal studies owing to their sensitivity to the toxic effects of $A\beta$ aggregates.³⁶ Originally developed by Mosmann, [3-(4,5-dimethylthiazol-2-yl)-2,5-diphenyltetrazolium]bromide (MTT) reduction is one of the most frequently used quantitative cell viability assay for measuring cell proliferation, neuronal cytotoxicity and cellular viability in drug screening.^{37,38}

PC-12 cells treated with 2 μ M of premonomerized $A\beta_{1-40}$ showed a robust decrease (31.2%) in their survival. Upon incubation with $A\beta_{1-40}$, only 68.8% cells were found to be viable. The viability of untreated cells was taken as 100. Since MTT is reduced by viable cells only, the reduction in the number of viable cells concomitantly results in the decrease in MTT reduction as observed by the OD₅₇₀ (optical density at 570 nm) measurements, indicating the cytotoxicity of $A\beta_{1-40}$ aggregates. In the cell viability assay, N-terminus free hexapeptide, Ile-Gly-Leu-Met-Val-Gly-NH₂ (**1**, IGLMVG-NH₂), was observed to fully protect the cells from the $A\beta_{1-40}$ -induced toxicity at a concentration of 2 μ M (1:1 ratio of $A\beta_{1-40}$ to **1**). When $A\beta_{1-40}$ was preincubated with the peptide **1** in the cell culture medium, the ability of the cells to metabolize MTT was dramatically restored to 100% (Figure 1). In the

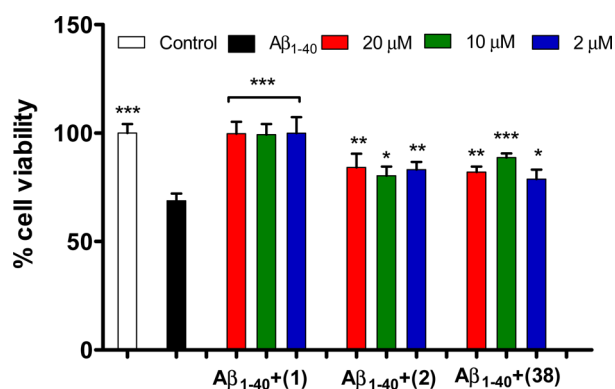


Figure 1. Effects of hexapeptides **1**, **2**, and **38** on the $A\beta_{1-40}$ -induced cytotoxicity in PC-12 cells. Cells were treated with $A\beta_{1-40}$ (2 μ M) alone or $A\beta_{1-40}$ plus **1**, **2**, or **38** (2–20 μ M) for 6 h, after which their ability to reduce MTT was measured. Control represents the untreated cell samples while $A\beta_{1-40}$ bar represents the cell viability upon treatment with $A\beta_{1-40}$ peptide. Subsequent bars represent the cell samples where the hexapeptides **1**, **2**, and **38** were coincubated along with $A\beta_{1-40}$ peptide. Viabilities are expressed as percentage of untreated cells (control). Experiments were done in triplicate. Error bars represent mean \pm standard deviation (SD, $n = 3$). Data were analyzed by one way anova test followed by Dunnett's multiple comparison test (* $p < 0.05$, ** $p < 0.01$, *** $p < 0.001$, Vs $A\beta_{1-40}$) using software (GraphPad Prism, ISI, San Diego, CA).

presence of this hexapeptide, no cell loss was observed, and the cell viability was found to be similar to that in the control (untreated cells). Total prevention of the inhibition of MTT reduction by peptide **1** indicates the complete inhibition of the $A\beta_{1-40}$ aggregation (Supporting Information (SI), Table S1). Two other hexapeptides, **2** (Val-Gly-Leu-Met-Val-Gly-NH₂, 20 μ M, Figure 1) and **38** (Ile-Gly-Leu-Met-Val-Nle-NH₂, 10 μ M, Figure 1), were also observed to restore cell viability significantly. The cell viabilities in the presence of these peptides were about 84.1 and 88.7, corresponding to about 49% and 63.7% inhibition of $A\beta_{1-40}$ aggregation, respectively (SI,

Table S1). While 10 other hexapeptides [(**4**, Aib-G-L-M-V-G-NH₂), (**10**, I-V-L-M-V-G-NH₂), (**16**, I-Nle-L-M-V-G-NH₂), (**18**, I-G-F-M-V-G-NH₂), (**28**, I-G-L-D-S-V-G-NH₂), (**29**, I-G-L-M-P-G-NH₂), (**30**, I-G-L-M-F-G-NH₂), (**33**, I-G-L-M-Aib-G-NH₂), (**39**, I-G-L-M-V-I-NH₂), and (**41**, I-G-L-M-V-V-NH₂)] were found to be moderately active and mitigated the $A\beta_{1-40}$ toxicity in the range of 21–40% in the tested concentration range (SI, Table S1). Rest of the tested hexapeptides exhibited very mild inhibitory activity (<20%, SI, Table S1). Cell viabilities in the presence of the hexapeptides **1**, **2**, and **38** relative to the control, at 2–20 μ M concentration range, are represented in Figure 1.

The hexapeptide, IGLMVG-NH₂ (**1**), that showed complete inhibition of $A\beta_{1-40}$ -induced toxicity was also checked for the inhibitory effects on the $A\beta_{1-42}$ peptide in the similar concentration range at the similar ratios (1:1, 1:5, and 1:10, $A\beta_{1-42}$: IGLMVG-NH₂). Similar to the study on $A\beta_{1-40}$, when the cells were treated with $A\beta_{1-42}$ in the presence of the peptide **1**, no signs of cytotoxicity were observed and the cell viability was similar to that of control samples (Figure 2). The cells were found to be fully rescued from the $A\beta_{1-42}$ aggregation-related toxicity in the presence of peptide **1**.

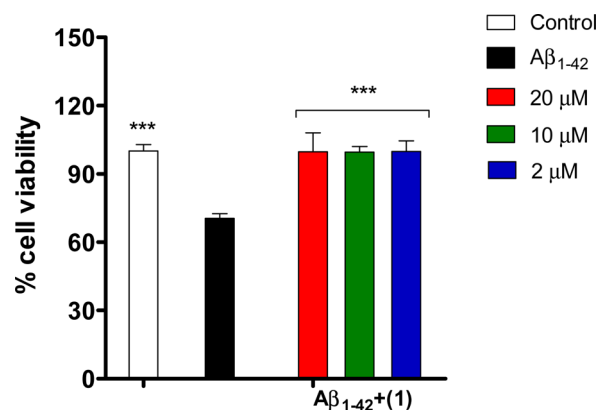


Figure 2. Effects of peptide **1** on the $A\beta_{1-42}$ -induced cytotoxicity in PC-12 cells. Cells were treated with $A\beta_{1-42}$ (2 μ M) alone or $A\beta_{1-42}$ plus **1** (2–20 μ M) for 6 h, after which their ability to reduce MTT was measured. Control represents the untreated cell samples while $A\beta_{1-42}$ bar represents the cell viability upon treatment with $A\beta_{1-42}$ peptide. Subsequent bars represent the cell samples where peptide **1** was coincubated along with the $A\beta_{1-42}$ peptide. Viabilities are expressed as percentage of untreated control. Experiments were done in triplicates. Error bars represent mean \pm standard deviation (SD, $n = 3$). Data were analyzed by one way anova test followed by Dunnett's multiple comparison test (* $p < 0.05$, ** $p < 0.01$, *** $p < 0.001$, Vs $A\beta_{1-42}$) using software (GraphPad Prism, ISI, San Diego, CA).

ThT Fluorescence Assay. The hexapeptide IGLMVG-NH₂ (**1**) was further tested for its inhibitory activity by thioflavin T (ThT) fluorescence assay against both the aggregating $A\beta$ sequences, $A\beta_{1-40}$ and $A\beta_{1-42}$. ThT, a cationic benzothiazole dye, has high affinity for the aggregated forms of amyloid proteins.³⁹ To investigate the effects of peptide **1** on $A\beta$ aggregation by ThT fluorescence assay, we first optimized the incubation conditions ($A\beta$ and ThT concentration, and time of incubation) and subsequently the optimized conditions were used in the studies. The results of the cell viability studies were well supported by ThT assay and a complete reduction in the ThT fluorescence was observed when the peptide **1** was coincubated with the $A\beta_{1-40}$ peptide. Taking the average of

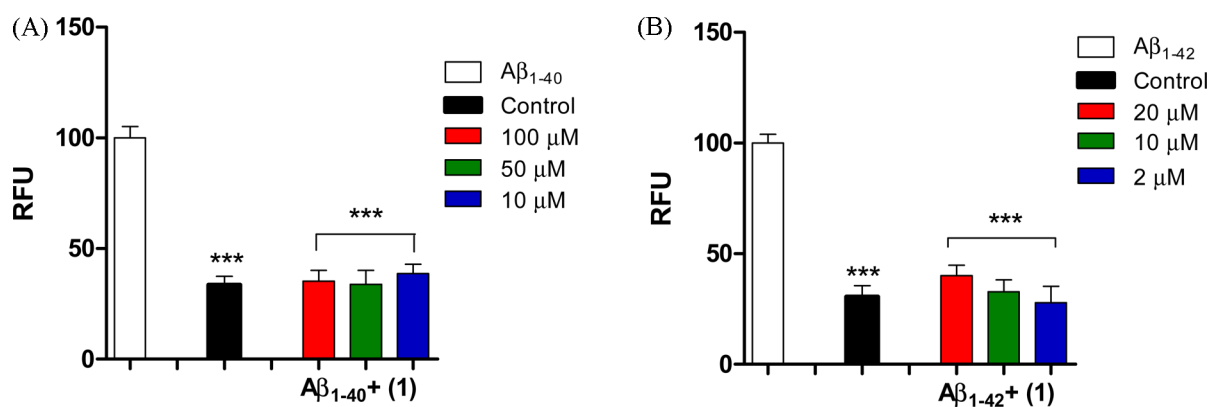


Figure 3. Effects of peptide 1 on (A) $A\beta_{1-40}$ and (B) $A\beta_{1-42}$ aggregation-mediated ThT fluorescence. Control sample represents the dye alone while the bars shown as $A\beta_{1-40}$ and $A\beta_{1-42}$ represent the corresponding $A\beta$ peptides incubated with the dye. Subsequent bars represent the peptide (1), coincubated with the corresponding $A\beta$ peptides at the described concentration ranges. RFU values for the $A\beta$ peptides coincubated with peptide 1 are expressed as percentage of the average fluorescence observed in $A\beta$ alone samples. Error bars represent mean \pm SD ($n = 3$). Data were analyzed by one-way ANOVA test followed by Dunnett's multiple comparison test ($*p < 0.05$, $**p < 0.01$, $***p < 0.001$, vs $A\beta$) using software (GraphPad Prism, ISI, San Diego, CA).

fluorescence observed in the $A\beta_{1-40}$ sample as 100, the relative fluorescence unit (RFU) values were calculated for the $A\beta_{1-40}$ peptide coincubated with 1 at the end of the incubation period. Figure 3A shows the bar graph representation of relative fluorescence units (RFUs) observed for the $A\beta_{1-40}$ peptide incubated alone, and $A\beta_{1-40}$ plus the peptide 1, relative to the ThT dye (control). ThT incubated alone exhibited a RFU value of 33.6% while in the presence of peptide 1, RFU values of 35.2%, 33.8%, and 38.6% were observed at 1:10, 1:5, and 1:1 ratios of $A\beta$: 1, respectively, corresponding to about 97.6, 99.7, and 92.5% inhibition of $A\beta_{1-40}$ aggregation. Similar to MTT assay, peptide 1 inhibited the aggregation of $A\beta_{1-42}$ peptide as indicated by the RFU values observed in the ThT measurements. When the peptide, IGLMVG-NH₂ was incubated with the $A\beta_{1-42}$ peptide, no enhancement in the ThT fluorescence was observed. The dye alone exhibited RFU of about 30.4, while in the presence of the peptide 1, RFU values of 40.1, 32.7, and 27.7 were observed, indicating complete absence of $A\beta_{1-42}$ aggregates. Figure 3B shows the graphical representation of the fluorescence values of the $A\beta_{1-42}$ peptide alone, and upon coincubation with the peptide 1, relative to the control.

Using ThT fluorescence measurement assay, we also studied the peptide 1 in a time-dependent manner against the $A\beta_{1-42}$ aggregation-mediated fluorescence. As shown in Figure 4, in the absence of the peptide 1, when $A\beta_{1-42}$ was aged alone with the ThT dye, there was a dramatic enhancement in the ThT fluorescence that could be ascribed to the aggregation state of the $A\beta_{1-42}$ peptide. A low fluorescence signal, initially for a period of 12 h represents the lag-phase indicating the absence of larger $A\beta$ aggregates. After 12 h, the rapid increase in the ThT fluorescence corresponds to the exponential-phase. The fluorescence reached a plateau in about 120 h. Taking the average of fluorescence observed in the $A\beta_{1-42}$ sample as 100, the relative fluorescence unit (RFU) values were calculated for the $A\beta_{1-42}$ peptide coincubated with peptide 1 at various time intervals. As shown in Figure 4, compared to the $A\beta_{1-42}$ sample, very low values of fluorescence were observed in the presence of peptide 1. The samples containing peptide 1 showed RFUs of 54%, 9%, 11.5%, 7.7%, and 9% at the time durations of 12, 24, 72, 120, and 168 h, respectively.

In the presence of peptide 1, very low RFU values ($\sim 10\%$) were observed especially once the fluorescence reached its

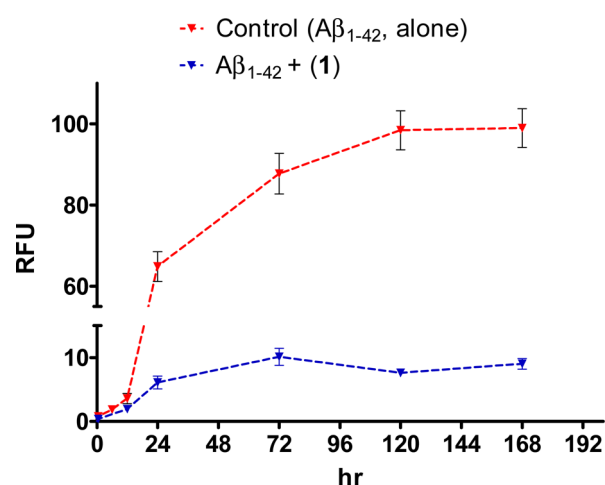


Figure 4. Effects of peptide 1 on $A\beta_{1-42}$ peptide aggregation, studied in a time-dependent manner for 7 days. Red colored line shows the $A\beta_{1-42}$ peptide aged alone. Blue line represents $A\beta_{1-42}$ peptide coincubated with peptide 1. Error bars represent mean \pm SD ($n = 3$). Data were analyzed by one way anova test followed by tukey's multiple comparison test ($**p < 0.01$, $***p < 0.001$) using software (GraphPad Prism, ISI, San Diego, CA).

saturation point (24–168 h). Since, the fluorescence values correspond to the aggregation state of the $A\beta$ peptides, complete retardation of fluorescence in the presence of peptide 1 clearly indicates its ability to interfere with the $A\beta_{1-42}$ peptide self-assembly. Since the peptide 1 retained its inhibitory effects on the $A\beta_{1-42}$ aggregation even after prolonged incubation, the results of the fluorometric analysis have been found in good agreement and correlated well with those obtained in the MTT-based assay with respect to the aggregation inhibitory activity of this hexapeptide.

Circular Dichroism Spectroscopy Study. $A\beta$ peptides that normally adopt conformation as a mixture of α -helix, β -sheet, and random coil in aqueous solution, undergoes a transition under abnormal conditions and aggregates in the form of intramolecular β -sheet structure. Circular dichroism (CD) spectroscopy provides a quantitative estimation of the various forms of secondary structure of proteins. The technique has been widely applied for the structural characterization of a

number of peptides/proteins in solution.⁴⁰ Promising results from MTT and ThT assay motivated us for further study on the peptide 1. We performed CD spectroscopy to analyze the secondary structural characteristics of the soluble $A\beta_{1-42}$ peptide aggregated alone, and in the presence of peptide 1. By CD spectroscopy, we investigated the effect of peptide 1 on the conformational transition of the $A\beta_{1-42}$ peptide by monitoring the residual molar ellipticity at 217 nm. β -Sheet of a peptide/protein is characterized by a negative ellipticity at 217 nm that further deepens as the β -sheet content increases.

The initial spectra of $A\beta_{1-42}$ peptide showed a high degree of unordered structure. When incubated alone, $A\beta_{1-42}$ showed a time-dependent spectral change from a minimum at 197 nm to development of a minimum at 217 nm, indicating transformation from unordered conformation to a β -sheet-rich structure (Figure 5). Initially, 61.8% of $A\beta_{1-42}$ peptide was in

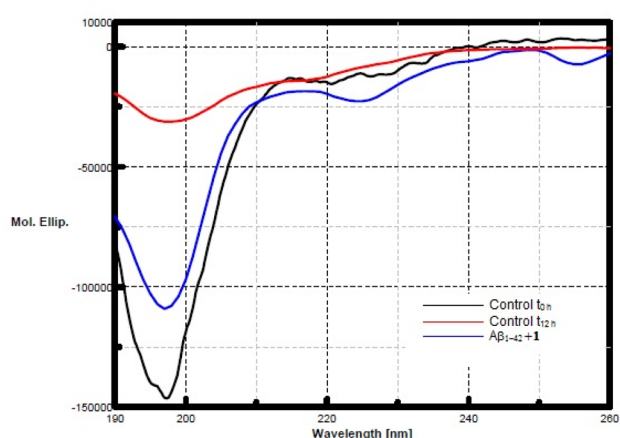


Figure 5. CD spectroscopic studies showing the inhibitory effects of peptide 1 on $A\beta_{1-42}$ aggregation. Differently colored curves show the $A\beta_{1-42}$ sample at t_{0h} (black), $A\beta_{1-42}$ sample at t_{12h} (red), and $A\beta_{1-42}$ peptide, coincubated with peptide 1 (blue) at t_{12h} .

random coil form, 28.7% in β -turn form with only 9.5% as β -sheet conformation; however, no α -helix conformation was observed. While at the end of incubation period, 47.1% of β -sheet component was observed, with only 42.3% of random coil structure. Though β -turn content was reduced to 10.6%, α -helix conformation was again not observed. To analyze the effect of the peptide 1 on the conformation of the $A\beta_{1-42}$ peptide, inhibitor spectrum was subtracted from the corresponding spectra of inhibitor-treated $A\beta_{1-42}$. In the presence of peptide 1, at the end of incubation period, only 16.8% of β -sheet was observed, with 59.3% of peptide still in random coil form. Reduction in β -sheet content was also visualized by the relatively shallower CD curve at 217 nm. Figure 5 depicts that when $A\beta_{1-42}$ was incubated alone, the minima at 217–218 nm deepens after 12 h (t_{12h} , red) compared to the 0 h (t_{0h}) curve (black), suggestive of an increase in β -sheet content. While in the presence of the peptide 1 (blue), no such minima was observed, demonstrating the inhibition of conformational transition. The prevention of conformational transition to β -sheet suggests the ability of the hexapeptide, IGLMVG-NH₂ to disrupt the aggregation process and lends further support the inhibitory effects of the peptide 1 as observed earlier in MTT and ThT assays.

High Resolution-Transmission Electron Microscopy (HR-TEM) and Scanning Transmission Electron Microscopy (STEM) Study.

Electron microscopy (EM) is a pivotal technique used to detect the presence of fibrils and further examine their morphology and size. The technique has been used to study a variety of proteins, including $A\beta$.⁴¹ Finally, we visually investigated the effects of peptide 1 on the morphology, size and abundance of $A\beta_{1-42}$ aggregates by high resolution transmission electron microscopy (HR-TEM) and scanning transmission electron microscopic analysis (STEM). Another hexapeptide 6, observed as inactive in the MTT cell viability assay, was taken as a negative control. After 72 h of incubation at 37 °C, numerous long and thick, rod-like cylindrical fibrils were observed when $A\beta_{1-42}$ peptide was incubated alone (Figure 6A, HR-TEM and Figure 7A, STEM) indicating its

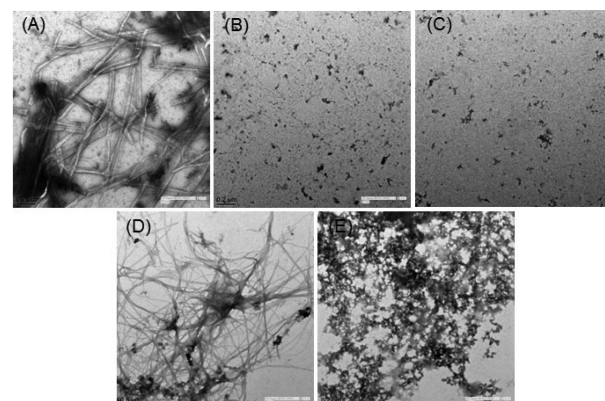


Figure 6. HR-TEM analysis of the effects of peptides 1 and 6 on the aggregation of $A\beta_{1-42}$ peptide. $A\beta_{1-42}$ was incubated (A) alone, and (B) with peptide 1, (D) with the peptide 6. Images (C) and (E) represent peptides 1 and 6, incubated alone, respectively. The scale bar shows 0.2 μm .

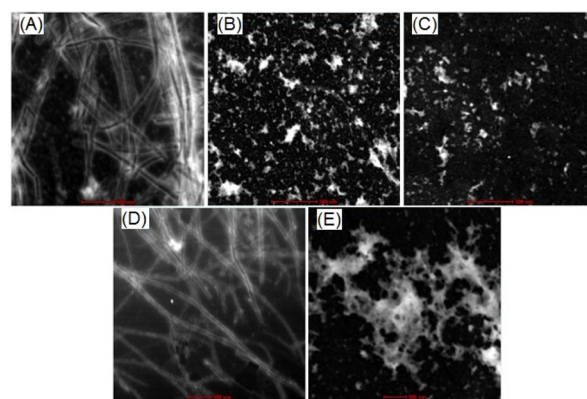


Figure 7. STEM analysis of the effects of peptides 1 and 6 on the aggregation of $A\beta_{1-42}$ peptide. $A\beta_{1-42}$ was incubated (A) alone, (B) with peptide 1, and (D) with peptide 6. Images (C) and (E) represent peptides 1 and 6, incubated alone, respectively. The scale bar shows 500 nm.

aggregation state. The structures extended to about 200–1000 nm in length and about 30–40 nm in width. While, upon incubation of $A\beta_{1-42}$ with the peptide 1, remarkable changes in the abundance and morphology of the $A\beta_{1-42}$ peptide structures were observed. The aggregates were completely disappeared when peptide 1 was coincubated with $A\beta_{1-42}$ peptide (Figure 6B, HR-TEM and Figure 7B, STEM) and only scarcely spread spherical particles were found all along the EM grid. Peptide 1 did not aggregate when incubated alone

under similar conditions and no fibrils were seen (Figure 6C, HR-TEM and Figure 7C, STEM), with only randomly scattered small spherical structures visible. However, in the presence of peptide 6 that was found inactive in cell culture studies, $A\beta_{1-42}$ was again observed to form an intense network of interconnecting clusters of aggregates (Figure 6D, HR-TEM and Figure 7D, STEM).

Peptide 6 was also found to self-aggregate and large network of nonfibrillar/amorphous aggregates were observed when it was incubated alone under similar conditions (Figure 6E, HR-TEM and Figure 7E, STEM). Such an observation again provides an explanation for its inefficiency as an amyloid aggregation inhibitor and supports the results of MTT assay.

Cytotoxicity Study. Being a part of the hydrophobic C-terminus of $A\beta$, the peptide 1 could aggregate and may be itself toxic to PC-12 cells. Thus, hexapeptide IGLMVG-NH₂ that showed 100% inhibition of amyloid aggregation was tested for the self-aggregation related toxicity by MTT cell viability assay. The similar procedure for sampling and assay was adopted as for the activity studies (SI). DMSO in the same concentration as in test wells was used as a control. The peptide 1 did not show any toxic effect on the cells under study at the highest tested concentration of 20 μ M (SI).

CONCLUSIONS

A full peptide scan on a hexapeptide fragment of $A\beta$ peptide resulted in the synthesis of more than 40 new peptides. Bioevaluation of these peptides as anti- $A\beta$ aggregation agents by cell culture-based and other assays led to the identification of a number of peptides that were observed to attenuate the $A\beta$ fibrillation in the range of 20–100%. Hexapeptide IGLMVG-NH₂ (1) was observed to completely rescue PC-12 cells from $A\beta$ aggregation-induced toxicity. Further confirmation of these results was made by ThT fluorescence assay. Secondary structural characteristics by CD spectroscopy and morphological examination by transmission electron microscopy were performed as a mean of final confirmation. Amino acid scanning strategy combined with other modifications may render peptidomimetics that may prove to be promising in treating the amyloid diseases. Suffice it to say, these short peptides may prove useful in the future drug development against AD and open a new avenue in research for treatment against brain disorders.

METHODS

Synthesis. All chemicals were purchased from Sigma-Aldrich (St. Louis, MO) and Chem-Impex International (Wood Dale, IL) and used without further purification, unless specified. All the solvents used for synthesis were of analytical grade and used without further purification, unless otherwise stated. Peptides were synthesized by using Aapptec Focus XC automated peptide synthesizer following solid phase peptide synthesis protocol (SPPS) using Fmoc chemistry on 0.1 mM scale. To synthesize C-terminal amidated peptides rink amide MBHA resin was used as solid support.

Resin was first swelled in DMF for 15 min in a reaction vessel equipped with a sintered glass bottom. Fmoc group on the linker was then removed by using 20% piperidine in DMF for 15 min (10 mL). Deprotection cycle was performed twice. Subsequently, Fmoc protected amino acid was first activated in situ by treatment with TBTU (3.0 equiv., 0.5 M in DMF) and DIEA (3.0 equiv., 1.0 M in DMF) and then coupled to the resin by mechanical shaking at ambient temperature for 2.5 h. In the case of aminoisobutyric acid (Aib), HATU was used as coupling reagent instead of TBTU. Successful completion of each coupling was routinely monitored by Kaiser's test.

The cycle of Fmoc removal and coupling was repeated with subsequent Fmoc protected amino acids to obtain resin-bound desired hexapeptides. Each coupling was followed by removal of Fmoc group and washing the resin by DMF. Cleavage of peptides from resin and concomitant deprotection of side chain protecting groups was carried out by using TFA/triisopropylsilane/water (95:3:2) as cleavage cocktail (15 mL/g), stirred magnetically at ambient temperature for 2.5 h. Filtration under vacuum afforded the peptide in filtrate. The volume of filtrate was reduced up to 0.5 mL. The crude peptides were precipitated by adding cold diethyl ether. Crude peptides were purified and were analyzed for purity by reverse-phase high performance liquid chromatography system and characterized for identity by high resolution mass spectroscopy (SI).

MTT Cell Viability Assay. To reproducibly monitor the $A\beta$ self-assembly, $A\beta$ peptides were first monomerized by TFA and HFIP treatments (SI). An aliquot of $A\beta$ peptides was taken and immediately before the experiment, 20 mM NaOH was added to make up a concentration of 200 μ M. The $A\beta$ peptides were diluted in 10 mM sodium phosphate buffer (pH 7.4) to 20 μ M. Cells in their exponential growth phase were seeded in 96-well plates, at a rate of 17 000 cells per well per 80 μ L, and were incubated overnight. Test peptides were dissolved in dimethyl sulfoxide (DMSO) as 5 mM stock solutions. Just before the experiments, test peptides were diluted in phosphate buffered saline (PBS) to the concentrations of 200, 100, and 20 μ M. Next morning, $A\beta$ (10 μ L) was added in each well with and without the test peptides (10 μ L). The final concentration of $A\beta$ was kept 2 μ M and that of test peptides as 2, 10, and 20 μ M so that their ratios were as 1:1, 1:5, and 1:10 ($A\beta$ /test peptides). The plates were incubated for 6 h. Untreated cell samples without $A\beta$ or test peptides with other components in the same concentration as in the test wells were taken as control. After 6 h, 20 μ L of MTT (5 mg/mL in PBS) was added in each well and incubated for 4 h. The plate was centrifuged at 4 °C for 10 min. Supernatant was carefully removed from the wells, and DMSO (200 μ L, per well) was added. The resulting suspension was mixed well, and OD₅₇₀ were measured. Statistical analysis was performed by one way anova test followed by Dunnett's multiple comparison test (* p < 0.05, ** p < 0.01, *** p < 0.001, Vs $A\beta$) using software (GraphPad Prism, ISI, San Diego, CA). P -Values less than 0.05 were considered as significant.

ThT Fluorescence Assay. Monomeric $A\beta_{1-40}$ was dissolved in 20 mM NaOH to obtain a concentration of 2 mM, and then diluted in sodium phosphate buffer (pH 7.4) to 100 μ M. A volume of 120 μ L of ThT (25 μ M), dissolved in glycine-NaOH buffer (pH 8.5) was added in each well of a black, 96-well plate with clear bottom. Peptide 1 was dissolved in DMSO at 5 mM stock and diluted in PBS to obtain concentrations of 1 mM, 500 μ M, and 100 μ M. A volume of 15 μ L of peptide 1 was added to each well, followed by the addition of 15 μ L of $A\beta_{1-40}$ to bring the final nominal concentrations of $A\beta_{1-40}$:1 in ratios of 1:1, 1:5, and 1:10. The plate was incubated for 72 h at 37 °C and shaken at 200 rpm. Plate was read at excitation and emission wavelengths of 445 and 485 nm, respectively. Except for the concentrations and the incubation periods, similar protocol was followed for the ThT study on $A\beta_{1-42}$ sequence. Statistical analysis was performed by one way anova test followed by dunnett's multiple comparison test (* p < 0.05, ** p < 0.01, *** p < 0.001, vs $A\beta$) using software (GraphPad Prism, ISI, San Diego, CA). P -Values less than 0.05 were considered as significant.

Time-Dependent ThT Assay. In the time-dependent study, peptide 1 was incubated with the $A\beta_{1-42}$ peptide and fluorescence was measured at regular intervals for a duration of 7 days. Inhibition activity was calculated by the relative percent enhancement in the RFU of the amyloid-bound ThT fluorescence of the target-inhibitor mixture compared to that in the absence of the inhibitor. The percentage inhibition of the $A\beta_{1-42}$ aggregation is given by $[1 - \{(Fb - Fc)/(Fa - Fc)\}] \times 100$, where Fa is the ThT fluorescence of the target peptide alone, Fb is the ThT fluorescence of the target-inhibitor complex, and Fc is the background ThT fluorescence with no target or inhibitor present.

CD Spectroscopy Study. Samples for circular dichroism study were prepared much like the thioflavin T assay with the only difference

being that trifluoroethanol (TFE) was used to dissolve peptide **1** in place of DMSO. $A\beta_{1-42}$ was dissolved in NaOH to a concentration of 200 μM and then diluted in sodium phosphate buffer to a concentration of 20 μM . The peptide **1** was dissolved in TFE and diluted in sodium phosphate buffer to concentration of 100 μM . Equal volumes of $A\beta_{1-42}$ and **1** were mixed to result in a concentration ratio of 1:5 ($A\beta_{1-42}/\mathbf{1}$) and incubated at 37 °C for 12 h ($t_{12\text{h}}$) in an eppendorf. The eppendorf tube was sealed tightly to avoid evaporation of TFE. The final CD spectrum for a given sample was determined by subtracting the buffer blank spectrum from that acquired for the sample. The far-UV CD spectra were smoothed by using the noise reduction option in the software. The direct CD measurements (θ , in mdeg) were converted to molar ellipticity, using $[\theta] = \theta / (10 \cdot C \cdot l)$, where C is the molar concentration (mol/L) and l is the path length. The molar ellipticity $[\theta]$ is in units, $\text{deg cm}^2 \text{dmol}^{-1}$. At least three scans were recorded for each run sample, and data were averaged. CD spectra were deconvoluted using software spectra manager II, and the relative percentages of various forms of secondary structures were calculated.

Transmission Electron Microscopy Study. An aliquot of $A\beta_{1-42}$ peptide was dissolved in 20 mM NaOH to make it 500 μM and then diluted in 10 mM sodium phosphate buffer (pH 7.4) to reach a concentration of 50 μM . The hexapeptides **1** and **6** (negative control) that were predissolved in DMSO at 5 mM concentration stock were diluted in sodium phosphate buffer to a final concentration of 250 μM . A volume of 25 μL of $A\beta_{1-42}$ was mixed with 25 μL of peptides **1** and **6**, so as to arrive at a concentration ratio of 1:5 ($A\beta_{1-42}/\text{test peptides}$). The solution was mixed well and incubated at 37 °C. After 72 h, 3–5 μL of sample was placed on a glow discharged grid. The sample was fixed on the grid by applying equal volume of 0.5% of glutaraldehyde solution by droplet procedure three to five times. The grid was washed with ultrapure water (3–5 μL) three times via single droplet method. Grids were negatively stained with 2% uranyl acetate. The sample was air-dried. Excess liquid was wicked away at every step using filter paper carefully through the grid edges, without letting the grid dry. At last, the grid was examined under the electron microscope. $A\beta_{1-42}$ alone plus the buffers in similar ratios and concentrations was used as a control. After incubation, fixation of peptide samples on the EM grid, washing, and staining were performed at 25 °C. Each EM grid was examined at several positions (>10) for the classification of fibril density and morphology.

■ ASSOCIATED CONTENT

● Supporting Information

The Supporting Information is available free of charge on the ACS Publications website at DOI: 10.1021/acscchemneuro.6b00006.

Chemistry: Purification method, characterization data (HPLC, purity and retention time; and HRMS), and HPLC chromatograms of few representative hexapeptides. Biological evaluation: Instruments and general methods for the MTT cell viability assay, thioflavin T fluorescence assay, circular dichroism spectroscopic and transmission electron microscopy is described in the Supporting Information. Bar graph showing cytotoxicity profile of peptide **1** and a zoomed section of CD spectrum, and the table showing the percentage inhibition data for all the hexapeptides. (PDF)

■ AUTHOR INFORMATION

Corresponding Author

*E-mail: rahuljain@niperr.ac.in.

Author Contributions

R.J. and S.B. conceptualized and experimentally designed this study. S.B. accomplished the peptide synthesis, purification/characterization, CD study and ThT assay under the super-

vision of R.J. The MTT assay and cytotoxicity study were accomplished by S.B., N.Y., and C.K.T. under the supervision of V.S.C. and R.J. TEM experiments were accomplished by S.B., I.K.M., and V.K. under the supervision of R.J. and K.T. The manuscript was written by R.J., S.B. and V.S.C.

Funding

S.B. thanks the Council of Scientific and Industrial Research, New Delhi, India, for the award of senior research fellowship.

Notes

The authors declare no competing financial interest.

■ ABBREVIATIONS

$A\beta$, amyloid beta peptide; AD, Alzheimer's disease; AChE, acetyl cholinesterase; APP, amyloid precursor protein; CD, circular dichroism; DIEA, diisopropylethylamine; DMF, *N,N*-dimethylformamide; DMSO, dimethyl sulfoxide; EGCG, epigallocatechin-3-gallate; EM, electron microscopy; FDA, Food and Drug Administration; Fmoc, 9-fluorenylmethoxycarbonyl; HATU, 1-[bis(dimethylamino)methylene]-1*H*-1,2,3-triazolo[4,5-*b*]pyridinium 3-oxidhexafluorophosphate; HFIP, hexafluoroisopropanol; HR-TEM, high resolution transmission electron microscopy; MBHA, 4-methylbenzhydrylamine; MTT, 3-(4,5-dimethylthiazol-2-yl)-2,5-diphenyltetrazolium bromide; NMDA, *N*-methyl-D-aspartate; OD, optical density; PC-12 cells, pheochromocytoma-12 cells; RFU, relative fluorescence unit; SD, standard deviation; SI, Supporting Information; STEM, scanning transmission electron microscopy; TBTU, *O*-(benzotriazol-1-yl)-*N,N,N',N'*-tetramethyluronium tetrafluoroborate; TFA, trifluoroacetic acid, ThT, thioflavin T

■ REFERENCES

- (1) Stelzmann, R. A., Schnitzlein, H. N., and Murtagh, F. R. (1995) An English translation of Alzheimer's 1907 paper, "über eine eigenartige erkrankung der hirnrinde." *Clin. Anat.* 8, 429–431.
- (2) Prince, M., Albanese, E., Guerchet, M., and Prina, M. (2014) *Dementia and risk reduction: An analysis of protective and modifiable factors*, Alzheimer's Disease International, London, <http://www.alz.co.uk/research/WorldAlzheimerReport2014.pdf>.
- (3) Selkoe, D. J. (1997) Alzheimer's Disease: genotypes, phenotype, and treatments. *Science* 275, 630–631.
- (4) Haass, C., and Selkoe, D. J. (1993) Cellular processing of β -amyloid precursor protein and the genesis of amyloid β -peptide. *Cell* 75, 1039–1042.
- (5) Eisenberg, D., and Jucker, M. (2012) The amyloid state of proteins in human diseases. *Cell* 148, 1188–1203.
- (6) Roberson, E. D., and Mucke, L. (2006) 100 years and counting: prospects for defeating Alzheimer's disease. *Science* 314, 781–784.
- (7) Vellas, B., Sol, O., Snyder, P., Ousset, P., Haddad, R., Maurin, M., Lemarié, J.-C., Désiré, L., and Pando, M. (2011) EHT0202 in Alzheimer's disease: A 3-month, randomized, placebo-controlled, double-blind study. *Curr. Alzheimer Res.* 8, 203–212.
- (8) Merck.ClinicalTrials.gov [website on the Internet] Bethesda, MD: US national library of medicine; 2013. [Accessed November 22, 2013]. Efficacy and safety trial of MK-8931 in participants with prodromal Alzheimer's disease (MK-8931-019) (APECS) [updated November 19, 2013]. Available from: <http://www.clinicaltrials.gov/ct2/show/NCT01953601?term=MK-8931&rank=3>. NLM identifier: NCT01953601.
- (9) Doody, R. S., Raman, R., Farlow, M., Iwatsubo, T., Vellas, B., Joffe, S., Kieburtz, K., He, F., Sun, X., Thomas, R. G., Aisen, P. S., et al. (2013) A phase III trial of semagacestat for treatment of Alzheimer's disease. *N. Engl. J. Med.* 369, 341–350.
- (10) Wilcock, G. K., Black, S. E., Balch, A. H., Amato, D. A., Beelen, A. P., Schneider, L. S., Green, R. C., Swabb, E. A., and Zavitz, K. H. (2009) Safety and efficacy of tarenfluril in subjects with mild

Alzheimer's disease: Results from an 18-month international multi-center phase III trial. *Alzheimer's Dementia* 5, 86.

(11) Coric, V., Salloway, S., van Dyck, C. V., Kerselaers, W., Kaplita, S., Curtis, C., Ross, J., Richter, R. W., Andreasen, N., Brody, M., Sharma, S. K., Cedarbaum, J. M., and Berman, R. (2013) A phase II study of the γ -secretase inhibitor avagacestat (BMS-708163) in prodromal Alzheimer's disease. *Alzheimer's Dementia* 9, 283.

(12) Holmes, C., Boche, D., Wilkinson, D., Yadegarfar, G., Hopkins, V., Bayer, A., Jones, R. W., Bullock, R., Love, S., Neal, J. W., Zotova, E., and Nicoll, J. A. (2008) Long-term effects of $A\beta_{1-42}$ immunization in Alzheimer's disease: Follow-up of a randomised, placebo-controlled phase I trial. *Lancet* 372, 216–223.

(13) Blennow, K., Zetterberg, H., Rinne, J. O., Salloway, S., Wei, J., Black, R., Grundman, M., and Liu, E. (2012) Effect of immunotherapy with bapineuzumab on cerebrospinal fluid biomarker levels in patients with mild-to-moderate Alzheimer disease. *Arch. Neurol.* 69, 1002–1010.

(14) Ritchie, C. W., Bush, A. I., Mackinnon, A., Macfarlane, S., Mastwyk, M., MacGregor, L., Kiers, L., Cherny, R., Li, Q. X., Tammer, A., Carrington, D., Mavros, C., Volitakis, I., Xilinas, M., Ames, D., Davis, S., Beyreuther, K., Tanzi, R. E., and Masters, C. L. (2003) Metal-protein attenuation with iodochlorhydroxyquin (clioquinol) targeting $A\beta$ amyloid deposition and toxicity in Alzheimer disease: A pilot phase II clinical trial. *Arch. Neurol.* 60, 1685–1691.

(15) Lannfelt, L., Blennow, K., Zetterberg, H., Batsman, S., Ames, D., Harrison, J., Masters, C. L., Targum, S., Bush, A. I., Murdoch, R., Wilson, J., and Ritchie, C. W. (2008) Safety, efficacy, and biomarker findings of PBT2 in targeting $A\beta$ as a modifying therapy for Alzheimer's disease: A phase IIa, double-blind, randomised, placebo-controlled trial. *Lancet Neurol.* 7, 779–786.

(16) Safety and efficacy study evaluating TRx0237 in subjects with mild-to-moderate Alzheimer's disease. <https://www.clinicaltrials.gov/ct2/show/NCT01689233>.

(17) Gozes, I., Morimoto, B. H., Tiong, J., Fox, A., Sutherland, K., Dangoor, D., Holser-Cochav, M., Vered, K., Newton, P., Aisen, P. S., Matsuoka, Y., Dyck, C. H., and Thal, L. (2005) NAP: Research and development of a peptide derived from activity-dependant neuro-protective protein (ADNP). *CNS Drug Rev.* 11, 353–368.

(18) Puzzo, D., Privitera, L., Leznik, E., Fa, M., Staniszewski, A., Palmeri, A., and Arancio, O. (2008) Picomolar amyloid- β positively modulates synaptic plasticity and memory in hippocampus. *J. Neurosci.* 28, 14537–14545.

(19) Yang, F. S., Lim, G. P., Begum, A. N., Ubeda, O. J., Simmons, M. R., Ambegaokar, S. S., Chen, P. P., Kaye, R., Glabe, C. G., Frautschy, S. A., and Cole, G. M. (2005) Curcumin inhibits formation of amyloid- β oligomers and fibrils, binds plaques, and reduces amyloid *in vivo*. *J. Biol. Chem.* 280, 5892–5901.

(20) Nakagami, Y., Nishimura, S., Murasugi, T., Kaneko, I., Meguro, M., Marumoto, S., Kogen, H., Koyama, K., and Oda, T. (2002) A novel β -sheet breaker, RS-0406, reverses amyloid β -induced cytotoxicity and impairment of long-term potentiation *in vitro*. *Br. J. Pharmacol.* 137, 676–682.

(21) Porat, Y., Abramowitz, A., and Gazit, E. (2006) Inhibition of amyloid fibril formation by polyphenols: Structural similarity and aromatic interactions as a common inhibition mechanism. *Chem. Biol. Drug Des.* 67, 27–37.

(22) Aisen, P. S., Gauthier, S., Ferris, S. H., Saumier, D., Haine, D., Garceau, D., Duong, A., Suh, J., Oh, J., Lau, W. C., and Sampalis, J. (2011) Tramiprosate in mild-to-moderate Alzheimer's disease—A randomized, double-blind, placebo-controlled, multi-centre study (the Alphase Study). *Arch. Med. Sci.* 1, 102–111.

(23) Salloway, S., Sperling, R., Keren, R., Porsteinsson, A. P., van Dyck, C. H., Tariot, P. N., Gilman, S., Arnold, D., Abushakra, S., Hernandez, C., Crans, G., Liang, E., Quinn, G., Bairu, M., Pastrak, A., and Cedarbaum, J. D. (2011) A phase II randomized trial of ELND005, scyllo-inositol, in mild-to-moderate Alzheimer disease. *Neurology* 77, 1253–1262.

(24) Mahler, A., Mandel, S., Lorenz, M., Ruegg, U., Wanker, E. E., Boschmann, M., and Paul, F. (2013) Epigallocatechin-3-gallate: A

useful, effective and safe clinical approach for targeted prevention and individualised treatment of neurological diseases? *EPMA Journal* 4, 5.

(25) Kokkoni, N., Stott, K., Amijee, H., Mason, J. M., and Doig, A. J. (2006) *N*-Methylated peptide inhibitors of β -amyloid aggregation and toxicity. Optimization of the inhibitor structure. *Biochemistry* 45, 9906–9918.

(26) Grillo-Bosch, D., Carulla, N., Cruz, M., Sánchez, L., Pujol-Pina, R., Madurga, S., Rabanal, F., and Giral, E. (2009) Retro-enantiomeric *N*-methylated peptides as amyloid aggregation inhibitors. *ChemMedChem* 4, 1488–1494.

(27) Gordon, D. J., Sciarretta, K. L., and Meredith, S. C. (2001) Inhibition of $A\beta_{1-40}$ fibrillogenesis and disassembly of $A\beta_{1-40}$ fibrils by short β -amyloid congeners containing *N*-methyl amino acids at alternate residues. *Biochemistry* 40, 8237–8245.

(28) Matharu, B., El-Agnaf, O., Razvi, A., and Austen, B. M. (2010) Development of retro-inverso peptides as anti-aggregation drugs for β -amyloid in Alzheimer's disease. *Peptides* 31, 1866–1872.

(29) Chacon, M. A., Barria, M. I., Soto, C., and Inestrosa, N. C. (2004) β -sheet breaker peptide prevents $A\beta$ -induced spatial memory impairments with partial reduction of amyloid deposits. *Mol. Psychiatry* 9, 953–961.

(30) Granic, I., Masman, M. F., Mulder, K. C., Nijholt, I. M., Naude, P. J. W., Haan, A. D., Borbély, E., Penke, B., Luiten, P. G. M., and Eisel, U. L. M. (2010) Leu-Pro-Tyr-Phe-Asp-NH₂ neutralizes $A\beta$ -induced memory impairment & toxicity. *J. Alzheimer's Dis.* 19, 991–1005.

(31) Jhee, S. S. (2003) *Single dose escalation study of PPI-1019, an $A\beta$ aggregation inhibitor*, New Clinical Drug Evaluation Unit, Boca Raton, FL.

(32) Fradinger, E. A., Monien, B. H., Urbanc, B., Lomakin, A., Tan, M., Li, H., Spring, S. M., Condrón, M. M., Cruz, L., Xie, C. W., Benedek, G. B., and Bitan, G. (2008) C-Terminal peptides co-assemble into $A\beta_{1-42}$ oligomers and protect neurons against $A\beta_{1-42}$ -induced neurotoxicity. *Proc. Natl. Acad. Sci. U. S. A.* 105, 14175–14180.

(33) Pratim Bose, P., Chatterjee, U., Nerelius, C., Govender, T., Norström, T., Gogoll, A., Sandegren, A., Göthelid, E., Johansson, J., and Arvidsson, P. I. (2009) Poly-*N*-methylated amyloid β -peptide ($A\beta$) C-terminal fragments reduce $A\beta$ toxicity *in vitro* and in *Drosophila melanogaster*. *J. Med. Chem.* 52, 8002–8009.

(34) Jarrett, J. T., Berger, E. P., and Lansbury, P. T., Jr (1993) The carboxy terminus of the amyloid protein is critical for the seeding of amyloid formation: Implications for the pathogenesis of Alzheimer's disease? *Biochemistry* 32, 4693–4697.

(35) Hilbich, C., Kisters-Woike, B., Reed, J., Masters, C. L., and Beyreuther, K. (1992) Substitutions of hydrophobic amino acids reduce the amyloidogenicity of Alzheimer's disease $A\beta$ peptides. *J. Mol. Biol.* 228, 460–473.

(36) Shearman, M. S., Ragan, C. I., and Iversen, L. L. (1994) Inhibition of PC-12 cell redox activity is a specific, early indicator of the mechanism of β -amyloid-mediated cell death. *Proc. Natl. Acad. Sci. U. S. A.* 91, 1470–1474.

(37) Mosmann, T. (1983) Rapid colorimetric assay for cellular growth and survival: Application to proliferation and cytotoxicity assays. *J. Immunol. Methods* 65, 55–56.

(38) Liu, Y., Peterson, D. A., Kimura, H., and Schubert, D. (1997) Mechanism of cellular 3-(4,5-dimethylthiazol-2-yl)-2,5-diphenyltetrazolium bromide (MTT) reduction. *J. Neurochem.* 69, 581–593.

(39) LeVine, H. (1993) Thioflavine T interaction with synthetic Alzheimer's disease β -amyloid peptides: Detection of amyloid aggregation in solution. *Protein Sci.* 2, 404–410.

(40) Alder, A. J., Greenfield, N. J., and Fasman, G. D. (1973) Circular dichroism and optical rotatory dispersion of proteins and polypeptides. *Methods Enzymol.* 27, 675–735.

(41) Petkova, A. T., Leapman, R. D., Guo, Z., Yau, W. M., Mattson, M. P., and Tycko, R. (2005) Self-propagating, molecular-level polymorphism in Alzheimer's β -amyloid fibrils. *Science* 307, 262–265.